Acknowledgment

This work was completed during the author's sabbatical in Germany under the auspices of the von Humboldt Stiftung. The design techniques described in this paper are patent pending. Commercial use of these methods require permission from the State University of New York at Buffalo.

References

[1] Smith, O. J. M., 1957, "Posicast Control of Damped Oscillatory Systems," *Proc. of the IRE*, pp. 1249–1255.
[2] Singer, N. C., and Seering, W. P., 1990, "Preshaping Command Inputs to Reduce System Vibrations," ASME J. Dyn. Syst., Meas., Control, **112**, pp. 76–82.
[3] Swigert, C. J., 1980, "Shaped Torque Techniques," J. Guid. Control, **3**, pp. 460–467.
[4] Singh, T., and Vadali, S. R., 1993, "Robust Time-Delay Control," ASME J. Dyn. Syst., Meas., Control, **112**, No. 2A, pp. 303–306.
[5] Singh, T., and Vadali, S. R., 1995, "Robust Time-Delay Control of Multimode Systems," Int. J. Control, **62**, No. 6, pp. 1319–1339.
[6] Murphy, B. R., and Watanabe, I., 1992, "Digital Shaping Filters for Reducing Machine Vibrations," IEEE Trans. Rob. Autom., **8**, pp. 285–289.
[7] Singh, T., 2002, "Minimax Design of Robust Controllers for Flexible Systems," AIAA Journal of Guidance, Control and Dynamics, **25**, No. 5, pp. 868–875.
[8] Liu, Q., and Wie, B., 1992, "Robust Time-Optimal Control of Flexible Spacecraft," J. Guid. Control Dyn., **15**, No. 3, pp. 597–604.
[9] Singh, G., Kabamba, P. T., and McClamroch, N. H., 1990, "Bang-Bang Control of Flexible Spacecraft Slewing Maneuvers. Guaranteed Terminal Pointing Accuracy," J. Guid. Control Dyn., **13**, No. 2, pp. 376–379.
[10] Singh, T., and Vadali, S. R., 1994, "Robust Time-Optimal Control: A Frequency Domain Approach," J. Guid. Control Dyn., **17**, No. 2, pp. 346–353.
[11] Singh, T., 1995, "Fuel/Time Optimal Control of the Benchmark Problem," J. Guid. Control Dyn., **18**, No. 6, pp. 1225–1231.
[12] Hindle, T. A., and Singh, T., "Robust Minimum Power/Jerk Control of Maneuvering Structures," 2001, J. Guid. Control Dyn., **24**, No. 1A, pp. 816–826.
[13] Muenchhof, M., and Singh, T., 2002, "Desensitized Jerk Limited Time-Optimal Control of Multi-Input Systems," AIAA Journal of Guidance, Control and Dynamics, **25**, No. 3, pp. 474–481.
[14] Sungyung, Lim, Homer, D. Stevens, and Jonathan, P. How, 1999, "Input Shaping Design for Multi-Input Flexible Systems," ASME J. Dyn. Syst., Meas., Control, **121**(3), pp. 443–447.

Extended Influence Coefficient Method for Rotor Active Balancing During Acceleration

Shiyu Zhou
Department of Industrial Engineering, University of Wisconsin-Madison, Madison, WI 53706

Stephen W. Dyer
BalaDyne Corporation, 665 HighLand Drive, Ann Arbor, MI 48108

Kwang-keun Shin
Electrical & Controls Integration Lab, General Motors, P.O. Box 9055, Warren, MI 48090

Jianjun Shi
Dept. of Industrial and Operations Engineering, University of Michigan, Ann Arbor, MI 48109

Jun Ni
Department of Mechanical Engineering, University of Michigan, Ann Arbor, MI 48109

Imbalance-induced vibration of rotating machineries is an important factor limiting the performance and fatigue life of a rotor system. Particularly, the severe resonant vibration of a rotor when it passes through its critical speeds could damage the rotor system. To avoid this peak vibration, this paper presents an active balancing method to offset the imbalance of the rotor system during acceleration by using an electromagnetic balancer. In this method, "instantaneous" influence coefficients at different speeds are obtained and stored in a look-up table. Then, a gain scheduling strategy is adopted to suppress the imbalance-induced vibration during acceleration based on the "instantaneous" influence coefficient table. A comprehensive testbed is built to validate this scheme, and the validation results are presented. [DOI: 10.1115/1.1651533]

1 Introduction

Rotating machinery is commonly used in industries. Imbalance-induced vibration is an important factor limiting the performance and fatigue life of the rotating system. Many balancing procedures have been developed to suppress this imbalance-induced vibration. Among all these methods, off-line balancing methods [8] are widely adopted in practice. However, off-line balancing methods cannot be used if the distribution of imbalance and/or the effective imbalance change during operation. For example, in high speed machining, tool changes frequently happen during the operation of the machine. Different toolholder has different imbalance distribution. In order to overcome this limitation of off-line balancing, some researchers [3,4,6,7,10] tried to actively balance the rotating systems during operation using mass redistribution devices. All these methods require that the rotating speed of the rotor is constant. In some other cases, the balancing needs to be completed during speed-varying transient time in order to save time and get better performance. For example, in high-speed machining, the machining tool will be engaged in cutting as soon as the spindle reaches steady state speed. If an active balancing scheme is used on this machine, the balancing has to be done during the acceleration period to avoid increasing the cutting cycle time. Furthermore, the maximum vibration of a rotor usually occurs when it passes through its critical speeds. To avoid this hostile peak vibration, balancing during acceleration is needed.

Some technical challenges are associated with active balancing during acceleration. First, in the constant rotating speed case the imbalance-induced vibration only contains a single frequency (the rotating speed). Hence, a simple rotor model [2] can be used to develop the active balancing algorithm. However, in the acceleration case the overall dynamics of the rotor are excited. It can be shown that under certain conditions, the speed-varying transient response of a rotor system is quite different from the constant speed response [9,11]. A more comprehensive rotor model needs to be developed to depict the rotor system. Second, it is well known that the responses of rotor systems to imbalance are different at different rotating speeds. To successfully balance the rotor during speed transient period, we need a quick response actuator to catch up with the rotating speed change.

In this paper, an active balancing scheme that can balance the rotor-bearing system during acceleration period is presented. The actuator used in this research is a new type of mass redistribution device [1]. The mass redistribution of this balancer can be finished in fractions of a second. To describe the overall dynamics of the rotor system during acceleration period, influence coefficients at different speeds are obtained and stored in a look-up table. Then,

Contributed by the Dynamic Systems, Measurement, and Control Division of THE AMERICAN SOCIETY OF MECHANICAL ENGINEERS for publication in the ASME JOURNAL OF DYNAMIC SYSTEMS, MEASUREMENT, AND CONTROL. Manuscript received by the ASME Dynamic Systems and Control Division February 11, 2003; final revision, June 25, 2003. Associate Editor: R. Mukherjee.

a gain scheduling strategy is used to suppress the imbalance-induced vibration during acceleration based on the influence coefficient table.

This paper consists of four sections. In Section 2, an algorithms used in active balancing scheme is introduced. In Section 3, the experimental validation procedure and the results are presented. Finally, conclusions are presented in Section 4.

2 The Active Balancing Algorithm

The influence coefficient method is a powerful off-line balancing method. The general formulation of the influence coefficient method is

$$\mathbf{v}=\mathbf{v}_0+\mathbf{C}\mathbf{w}. \tag{1}$$

In Eq. (1), $\mathbf{v}$, also called residue vibration, is an m by 1 complex vector representing the rotor synchronous vibration (both magnitude and phase) measured at m locations. Synchronous vibration is the vibration with the frequency of the rotor rotating speed. $\mathbf{v}_0$, also an m by 1 complex vector, represents the rotor synchronous vibration at the m sensor locations caused by the system inherent imbalance. $\mathbf{w}$ is a n by 1 complex vector representing the imbalances (both magnitude and location) provided by balancers at n locations. $\mathbf{C}$ is an m by n complex matrix whose elements are the influence coefficients relating the imbalances provided by balancers and the rotor synchronous vibration response. The influence coefficient is a function of the sensor/balancer position and the rotating speed. The assumptions behind Eq. (1) are that the rotor synchronous response is proportional to the imbalance and that the effect of individual imbalances can be superimposed to give the effect of a set of imbalances. These two assumptions have been generally accepted if the imbalances, and hence the imbalance-induced vibration, are not very large.

The estimation of $\mathbf{C}$ can be obtained by trial runs. First, the imbalance of the balancer is set as $\mathbf{w}_1$ and the corresponding vibration is measured as $\mathbf{v}_1$. Then, the imbalance of the balancer is set as $\mathbf{w}_2$, which is different from $\mathbf{w}_1$, and the corresponding vibration is $\mathbf{v}_2$. The influence coefficient is estimated as

$$\mathbf{C}^{ij}=\frac{\mathbf{v}_1^i-\mathbf{v}_2^i}{\mathbf{w}_1^j-\mathbf{w}_2^j} \tag{2}$$

where $\mathbf{C}^{ij}$ is the (i,j)th element of $\mathbf{C}$ matrix, $\mathbf{v}^i$ is the vibration at the ith measurement location, and $\mathbf{w}_j$ is the imbalance provided by the jth balancer.

To minimize the residue vibration $\mathbf{v}$, we have the control law

$$\mathbf{w}=-(\mathbf{C}^{\mathbf{T}}\mathbf{C})^{-1}\mathbf{C}^{\mathbf{T}}\mathbf{v}_0. \tag{3}$$

$\mathbf{w}$ is the least squares solution of $\mathbf{v}_0+\mathbf{C}\mathbf{w}=0$. In the control law Eq. (3), the influence coefficient matrix is obtained through experimental trial runs. Ideally, this control law only needs one movement if the pre-estimated influence coefficients are perfect and the vibration measurement is accurate. In practice, however, we need several control iterations to minimize the imbalance-induced vibration. For the kth iteration, we have

$$\mathbf{v_0}=\mathbf{v}_k-\mathbf{C}\mathbf{w}_k. \tag{4}$$

Considering Eqs. (3) and (4) yields

$$\mathbf{w}_{k+1}=\mathbf{w}_k-(\mathbf{C}^{\mathbf{T}}\mathbf{C})^{-\mathbf{1}}\mathbf{C}^{\mathbf{T}}\mathbf{v}_k. \tag{5}$$

This control law only works at constant rotating speed because the influence coefficients change with the rotating speed.

For the acceleration case, ‘‘instantaneous’’ influence coefficients can be used to extend this control law. It is known that the imbalance response of a rotor system without gyroscopic effects consists of three parts: a small transient vibration due to sudden acceleration, the synchronous vibration with the frequency of instantaneous rotating speed, and a suddenly occurring transient vibration [9]. If we neglect the non-synchronous transient vibration, the synchronous response for a general rotor system during acceleration can be obtained based on Eq. (22) in [9]

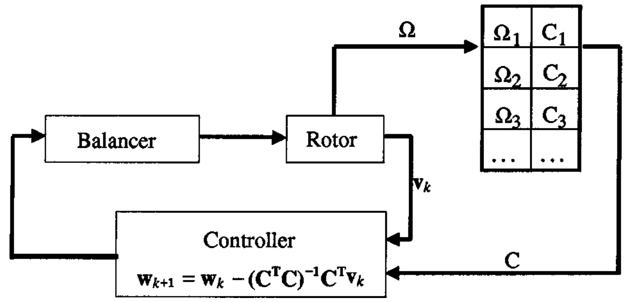

Fig. 1 Diagram of active balancing based on influence coefficient table

$$\mathbf{v}(t)=\mathbf{w}\sum_{k=1}^{N}\mathbf{u}_k[e^{i(\alpha t^2/2+\rho_k(t))}M_{sk}(t)]+\mathbf{v}_0(t), \tag{6}$$

where $\mathbf{v}(t)$ is a complex number that represents the overall synchronous vibration of rotor. It consists of two terms: (1) $\mathbf{v}_0(t)$ is the synchronous vibration caused only by the system inherent imbalance, and (2) the synchronous vibration caused by the balancer, where N is the number of significant vibration modes, $\mathbf{w}$ is the imbalance provided by the balancer in the balancer's coordinate system, $\mathbf{w}\cdot\mathbf{u}_k$ is a complex number that represents the imbalance provided by the balancer in the kth mode. α is the rotor acceleration. M_{sk} and ρ_k are defined as the magnitude and phase of the synchronous vibration in the kth mode when the imbalance provided by the balancer is one unit, respectively. Please note M_{sk} and ρ_k are only related with the dynamic parameters of the rotor system, not with the imbalance. If ‘‘instantaneous’’ influence coefficient is defined as

$$\mathbf{C}'(t)=\sum_{k=1}^{N}\mathbf{u}_k[e^{i[\alpha t^2/2+\rho_k(t)]}M_{sk}(t)], \tag{7}$$

then we have

$$\mathbf{v}(t)=\mathbf{w}\cdot\mathbf{C}'(t)+\mathbf{v}_0(t). \tag{8}$$

The ‘‘instantaneous’’ influence coefficient at different speeds can be obtained by only two acceleration trial runs. First, the rotor system can be accelerated from 0 rpm to working speed with the imbalance provided by the balancer as $\mathbf{w}_1$. The vibration signal during the acceleration is recorded as $\mathbf{v}_1(t)$. Then, we can change the balancer's position and let it provide imbalance as $\mathbf{w}_2$. The system can be accelerated again and the vibration signal is recorded as $\mathbf{v}_2(t)$. Finally, the ‘‘instantaneous’’ influence coefficient at the interested speed (or time) can be obtained by

$$\mathbf{C}'^{ij}(t)=\frac{\mathbf{v}_1^i(t)-\mathbf{v}_2^i(t)}{\mathbf{w}_1^j-\mathbf{w}_2^j} \tag{9}$$

Equation 9 is similar to Eq. 2 except that the instantaneous influence coefficient is time-varying. Based on the concept of the ‘‘instantaneous’’ influence coefficient, the influence coefficient balancing method can be extended to speed varying case. A diagram of this extension is shown in Fig. 1.

In Fig. 1, $\mathbf{v}_k$ is the rotor vibrations at the sensor positions, Ω is the current rotating speed, and $\mathbf{C}$ is the influence coefficient corresponding to current speed. $\mathbf{C}$ is picked from a predefined table that is obtained by experimental trial runs. If there is no exact match of Ω in the table, a linear interpolation can be used as follows.

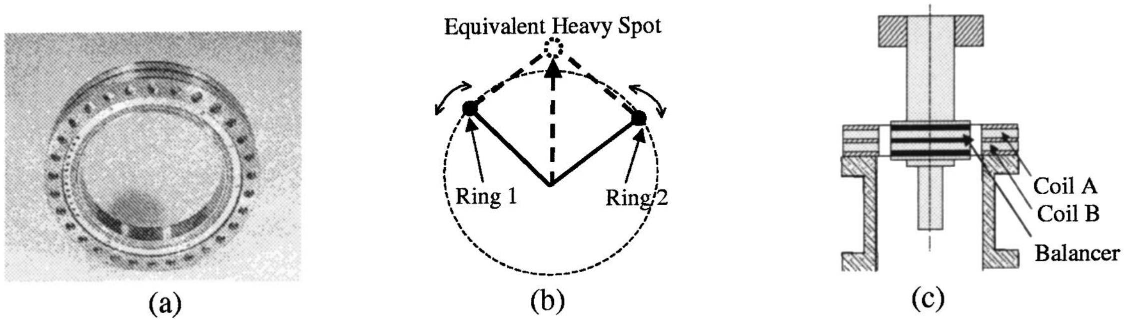

Fig. 2 The electromagnetic active balancer. (a) a photo of the electromagnetic balancer (b) a diagram of balancer's working principle (c) a diagram shows a balancer mounting on a toolholder and the coils that supplies powers for the balancer movement.

$$\mathbf{C}^{ij}=\mathbf{C}_k^{ij}+\frac{\Omega-\Omega_k}{\Omega_{k+1}-\Omega_k}(\mathbf{C}_{k+1}^{ij}-\mathbf{C}_k^{ij}) \tag{10}$$

where $\Omega_k \leqslant \Omega < \Omega_{k+1}$ and the superscript i, j is the matrix element index. The rationale for the element-wise interpolation of the influence coefficient matrix is that the (i,j)th element of $\mathbf{C}$ is roughly the magnitude and phase of the transfer function between the jth imbalance and the response at the ith sensor position evaluated at the given rotational speed. For a mechanical system, the transfer function should be smooth and, if the speed interval between Ω_{k+1} and Ω_k is small, the linear interpolation is a good approximation.

The control law used in Fig. 1 is related to the control law used by Knospe, et al. [5]. In their imbalance control scheme, the actuator is the magnetic bearing. Because the imbalance produces a rotating centrifugal force, a synchronous rotating force can be generated at the magnetic bearings to offset the centrifugal force. The magnitude and phase of the controlled synchronous force is decided based on the influence coefficient model of the rotor. Therefore, their control law is also an extension of the influence coefficient balancing method.

To successfully implement this active balancing scheme, two problems need to be addressed. First is the stability issue caused by the delay in the movement of the balancer. Assume we pick up an influence coefficient at step k, and the time of finishing the control iteration is at time step $k+1$. The difference between these two time steps is the delay caused by the algorithm and the balancer movement. Since the control law is implemented based on $\mathbf{C}_k$, the calculated imbalance at $k+1$ should be $\mathbf{w}_{k+1}=\mathbf{w}_k-(\mathbf{C}_k^T\mathbf{C}_k)^{-1}\mathbf{C}_k^T\mathbf{v}_k$. Therefore, the vibration at $k+1$ is

$$\mathbf{v}_{k+1}=\mathbf{C}_{k+1}\mathbf{w}_{k+1}+\mathbf{v}_0=\mathbf{C}_{k+1}(\mathbf{w}_k-(\mathbf{C}_k^T\mathbf{C}_k)^{-1}\mathbf{C}_k^T\mathbf{v}_k)+\mathbf{v}_0. \tag{11}$$

Noticing $\mathbf{v}_k=\mathbf{C}_k\mathbf{w}_k+\mathbf{v}_0$ and substituting it into Eq. (11), we get $\mathbf{v}_{k+1}=\mathbf{C}_{k+1}(\mathbf{w}_k-(\mathbf{C}_k^T\mathbf{C}_k)^{-1}\mathbf{C}_k^T(\mathbf{C}_k\mathbf{w}_k+\mathbf{v}_0))+\mathbf{v}_0$. Since $(\mathbf{C}_k^T\mathbf{C}_k)^{-1}\mathbf{C}_k^T\mathbf{C}_k\mathbf{w}_k=\mathbf{w}_k$, hence, we have

$$\mathbf{v}_{k+1}=(\mathbf{I}-\mathbf{C}_{k+1}(\mathbf{C}_k^T\mathbf{C}_k)^{-1}\mathbf{C}_k^T)\mathbf{v}_0 \tag{12}$$

To ensure efficient imbalance reduction, we need $\|\mathbf{v}_{k+1}\|<\|\mathbf{v}_0\|$, which means a sufficient condition for stability is

$$\bar{\sigma}(\mathbf{I}-\mathbf{C}_{k+1}(\mathbf{C}_k^T\mathbf{C}_k)^{-1}\mathbf{C}_k^T)<1, \tag{13}$$

where $\bar{\sigma}(\cdot)$ denotes the maximum singular value. The intuitive understanding can be obtained by considering the simplest one dimension case. In that case, the criterion tells that if the signs of $\mathbf{C}_{k+1}$ and $\mathbf{C}_k$ keep the same, the active balancing scheme will be effective. In this analysis, the uncertainty in the influence coefficient estimation is not considered. In practice, multiple trial runs and averaging can ensure the accuracy of the estimation. In most cases, we can neglect the difference between the true influence coefficients and the values in the look-up table.

The second problem needs to be addressed is the effect of the system damping. A very small system damping (the damping coefficient is less than 0.05 in our experience) could cause two problems in the active balancing: (i) significant nonsynchronous transient vibration will happen during acceleration period under small damping condition. The transient vibration will cause significant difficulties in the calculation of the synchronous vibration component, particularly when its frequency is close to the synchronous frequency. However, the synchronous vibration calculation is critical in both the influence coefficient estimation and the real-time implementation of the control law. Significant transient vibration will degrade the performance of influence coefficient method. (ii) the movement of the balancer could cause an undesired transient vibration under small damping condition. To deal with this problem, the balancing action should be avoided when the rotating speed is close to the critical speeds. The balancing region can be decided through experiments based on the engineering requirement on the tolerable transient vibration.

In general, small damping has a detrimental impact on the performance of the proposed active balancing method. Fortunately, for many machining tools, particularly for the belt-driven machining tools, the system damping is not small ($\zeta>0.05$). The impact of the transient vibration can be ignored. Based on this active balancing scheme, a hardware setup is built and experimental validation is conducted.

3 Experimental Validation

3.1 Introduction of the Electromagnetic Balancer. An electromagnetic balancer is used in this research. The working principle of this mass-redistribution balancer is shown in Fig. 2.

The balancer consists of two rings as shown in Fig. 2(*a*). These two rings are not balanced and can be viewed as two heavy spots as shown in Fig. 2(*b*). After mounted on the spindle or toolholder, the balancer can rotate with the rotor. These two rings are held in place by permanent magnetic forces. When the balancer is activated, an electric current passes through the coil as shown in Fig. 2(*c*), the rings can be moved with respect to the spindle by the electromagnetic force. There are two individual coils in one package. Hence, the two rings can be moved individually. The combination of these two heavy spots is equivalent to a single heavy spot as shown in Fig. 2(*b*). Moreover, two magnetic hall sensors are mounted on the two coils. Using these two sensors, we can detect the relative locations of these two rings with respect to the reference position. In this way, we can have feedbacks of the locations of the heavy spots.

3.2 The Experimental Setup. An experimental testbed was built on a Fadal (HS88) vertical machining center. A diagram and a photo of the testbed are shown in Fig. 3.

There are four types of sensor in the system: (1) An encoder disk mounted on the balancer and a transmissive optical sensor

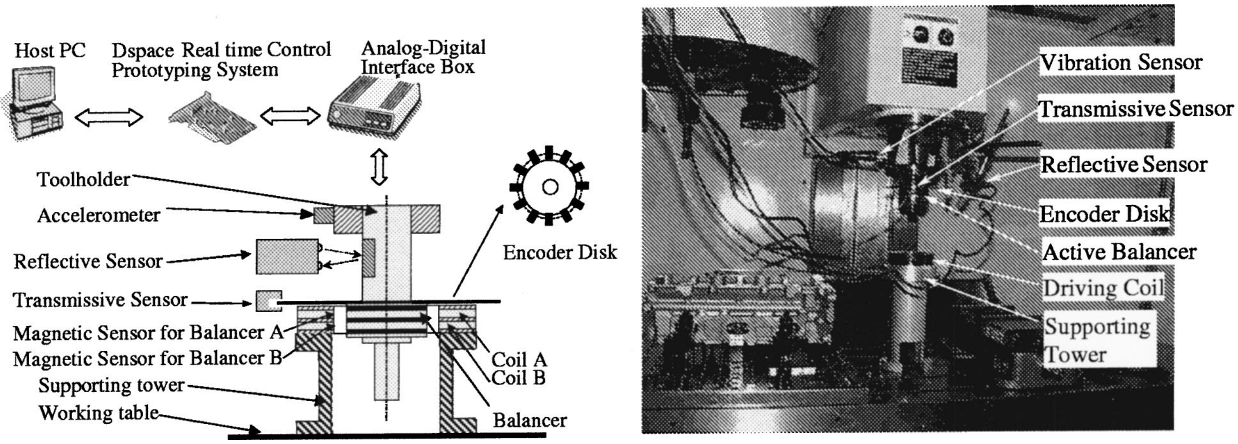

Fig. 3 The basic structure of the active balancing testbed

can generate 30 evenly distributed pulses per revolution. These pulses are used as the reference for the position and speed measurements. (2) A reflective optical sensor and a reflective tape attached on the spindle can generate one pulse per revolution. The rising edge of this pulse is used as the reference zero position. The positions of the rings of the balancer and the phase of the vibration are all with respect to this reference. (3) Two magnetic hall sensors detect the positions of the two rings of the balancer. (4) Rotor vibration is measured by accelerometer. This signal is an analog signal. It is sampled and converted into digital signal by an analog-to-digital converter. One point needs to be noticed is that the sampling of the vibration signal is triggered by the encoder signal. Therefore, the vibration signal is sampled at even spindle angle increments, instead of even time increments. The advantage of this sampling strategy is that the synchronous vibration can be easily estimated from this angle-based sampling signal. These signals are illustrated in Fig. 4.

3.3 Experimental Validation Results. To implement the active balancing scheme, an influence coefficient table needs to be obtained by trial runs. Define the imbalance provided by one balancer ring as one unit. Therefore, the maximum imbalance provided by the balancer is two units. The influence coefficient as a function of speed for the Fadal vertical machine center is shown in Fig. 5. The influence coefficients are obtained under the acceleration around 1,000 rpm/s. For this particular machine, the impact of different accelerations on the "instantaneous" influence coefficient is negligible.

The influence coefficients depict the transfer function of the rotor system from the excitation at the balancer position to the vibration at the sensor position. Clearly, the system can be viewed as a second-order dynamic system when the rotating speed is below 11,000 rpm. The resonant peak of the system occurs between 7,500~8,500 rpm.

The comparison between the system vibration with and without active balancing is shown in Fig. 6. Figure 6(*a*)~(*d*) show the active balancing performance under fast acceleration condition. The acceleration rate is from 4,000 to 10,000 rpm in 2 s. Figure 6(*a*) illustrates the synchronous vibration without active balancing. The speed profile is also shown in the figure. Figure 6(*b*) illustrates the synchronous vibration during fast acceleration with active balancing. It can be seen that the synchronous vibration is suppressed significantly. Figures 6(*c*) and 6(*d*) show the control action during the active balancing. Figure 6(*c*) illustrates the angular location of the rings of the balancer with respect to the reference location (the position of the reflective tape). Initially, the two rings are separated by 180 degree so that the balancer is self-balanced, which means no imbalance is provided by the balancer. Active balancing is activated by the magnitude of the synchronous vibration. If the magnitude is larger than 0.05 g, the active balancing scheme is activated. Furthermore, to avoid the impact of the movement of the balancer, the active balancing is deactivated when the rotating speed is between 7,500 rpm and 8,500 rpm. From Fig. 6(*c*), the balancer is activated several times during the whole acceleration period. Figure 6(*d*) illustrates the control actions in a polar coordinate system. The magnitude and the phase of the overall imbalance provided by the two rings are illustrated. There are two significant jumps in the whole control action.

Figures 6(*e*)~(*g*) illustrate the active balancing performance under slow acceleration condition. A slow acceleration from 4,000 rpm to 10,000 rpm within 10 s is used. The imbalance-induced vibration is also suppressed significantly during the acceleration

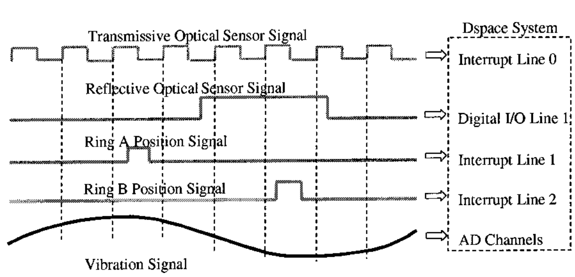

Fig. 4 The signal diagram of the active balancing experiment

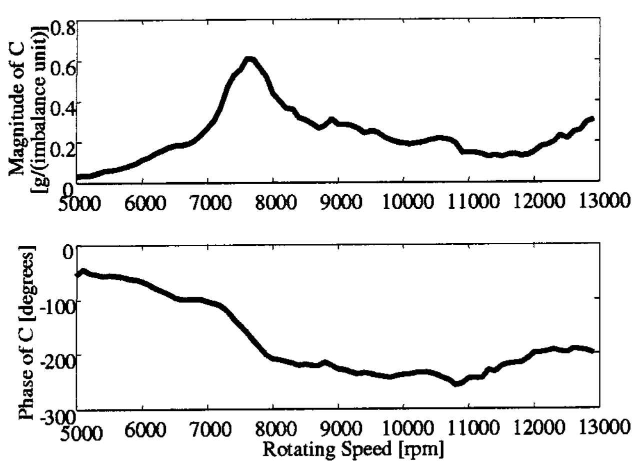

Fig. 5 The influence coefficients of fadal machine center at various speeds

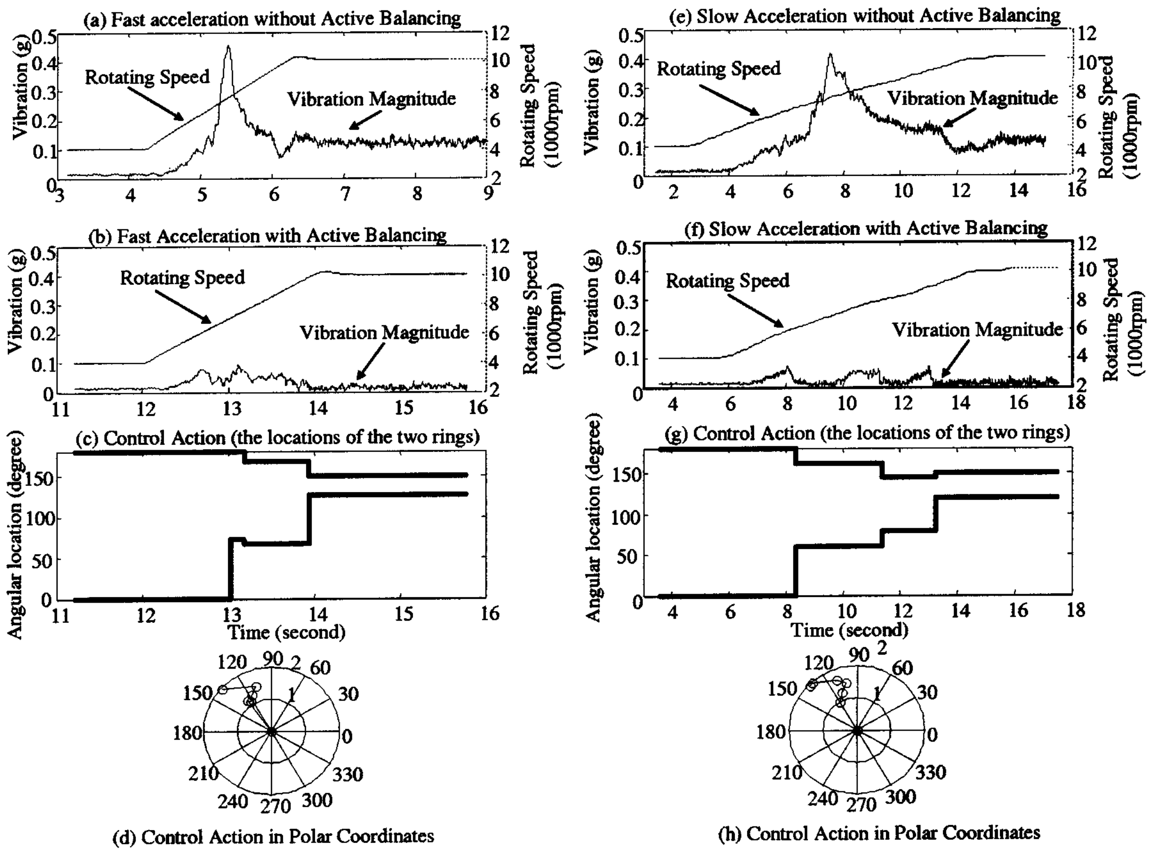

Fig. 6 Experimental validation results

period. Since the balancer has enough time to respond to the system vibration during slow acceleration period, the hostile vibration at the resonant peak is almost eliminated completely. This observation has significant engineering implications. During the startup of turbomachineries used in chemical or energy industries, the acceleration is often very slow. The most difficult task during the startup is to pass the critical speeds. The experimental results demonstrated indicate that active balancing during acceleration period can be used to eliminate the hostile peak vibrations during the start-up period. Hence, this technology can find extremely wide applications in practice.

4. Conclusions

This paper addresses the problem of active balancing during acceleration period. This problem is dealt by a gain scheduling strategy. The experimental validation shows the effectiveness of this strategy. This technology can be used widely in high speed machining tools, turbomachineries, etc.. There are still several open issues in this scheme. In this article, we studied the stability issue caused by the delay of the balancer movement. However, the stability will also be affected by the estimation error of the instantaneous influence coefficients and the synchronous vibration. In practice, the instantaneous influence coefficients can be estimated through the average of multiple trial runs to reduce the estimation error. However, the estimation of the synchronous vibration is a complicated issue. When the rotating speed hits the natural frequency, the transient vibration cannot be neglected if the damping of the rotor system is small. This might cause difficulties in the application of this strategy. Another issue is the optimal placement of the sensors and balancers. It is well-known that the location of the balancer will affect the magnitude of the influence coefficients. How to layout the sensors and the balancers to achieve the best control performance is an important engineering problem. These issues are currently under investigation. The results will be reported in the near future.

Acknowledgments

This work was supported by BalaDyne Corporation and the U.S. Department of Commerce, National Institute of Standards and Technology, Advanced Technology Program, Cooperative Agreement Number 70NANB7H3029.

References

[1] Dyer, S. W., Hackett, B. K., and Kerlin, J., 1998, "Electromagnetically Actuated Rotating Imbalance Compensator," *U.S. Patent No. 5757662*, Issued May 26, 1998.

[2] Goodman, T. P., 1964, "A Least-Squares Method for Computing Balance Corrections," ASME J. Eng. Ind., August, pp. 273–279.

[3] Gosiewski, Z., 1985, "Automatic Balancing of Flexible Rotors, Part 1: Theoretical Background," J. Sound Vib., **100**(4), pp. 551–567.

[4] Gosiewski, Z., 1987, "Automatic Balancing of Flexible Rotors, Part 2: Synthesis of System," J. Sound Vib., **114**(1), pp. 103–119.

[5] Knospe, C. R., Hope, R. W., Tamer, S. M., and Fedigan, S. J., 1996, "Robustness of Adaptive Imbalance Control of Rotors with Magnetic Bearings," J. Vib. Control, **2**, 352.

[6] Van De Vegte, J., and Lake, R. T., 1978, "Balancing of Rotating Systems During Operation," J. Sound Vib., **57**(2), pp. 225–235.

[7] Van De Vegte, J., 1981, "Balancing of Flexible Rotors During Operation," J. Mech. Eng. Sci., **23**(5), pp. 257–261.

[8] Wowk, V., 1995, "Machinery Vibration: Balancing," *McGraw-Hill, Inc.* New York.

[9] Zhou, S., and Shi, J., 2001, "The Analytical Unbalance Response of Jeffcott Rotor during Acceleration," ASME Transactions, ASME J. Manuf. Sci. Eng., **123**, pp. 299–302.

[10] Zhou, S., and Shi, J., 2001, "Active Balancing and Vibration Control of Rotating Machinery: A Survey," Shock Vib. Dig., **33**(5), pp. 361–371.

[11] Zhou, S., and Shi, J., 2001, "Imbalance Estimation for Speed-Varying Rigid Rotors Using Time-Varying Observer," ASME Transactions, ASME J. Dyn. Syst., Meas., Control, **123**, pp. 637–644.